

Boundary layer control using porous lamination

Aswathy Nair K.* and A. Sameen

Department of Aerospace Engineering, Indian Institute of Technology Madras, Chennai, India

* aswathynairk90@gmail.com

Abstract

The effect of porous lamination on zero pressure gradient flow over a flat plate is analysed using experiments from a separation control perspective. The porous lamination is modeled as an array of cylinders placed downstream of a backward facing step. The porosity of the lamination, ϕ , is calculated using the distance between the cylinders and values of $\phi = 0.65$ and 0.8 are studied at $Re = 391, 497$ and 803 , based on the characteristic length of the porous lamination and the free stream velocity in the wind tunnel. The temporal ($\bar{\cdot}$) and Representative Elementary Volume averaged ($\langle \cdot \rangle$) values of the flow properties are compared with those for the flat plate boundary layer flow to comprehend the influence of the porous layer. The flow dynamics at the fluid-porous interface is investigated with focus on the interfacial slip velocity, U_{slip} , and its dependence on ϕ and Re . The velocity measurements confirmed the existence of a non-zero slip velocity at the fluid-porous interface, by virtue of the porous lamination. $\langle \bar{U}_{slip} \rangle$ was found to increase with ϕ and Re . A passive suction-blowing velocity was also observed at the fluid-porous interface at higher ϕ and Re , which resulted in flatter velocity profiles over the porous lamination. Numerical analysis is carried out to analyse the ϕ and Re outside the scope of the experimental investigation and provided necessary data to substantiate the experimental analysis. The presence of the slip wall and the flatter velocity profiles suggest a stabilization of the flow and indicate separation delay. Hence, we propose the use of porous lamination as a passive separation control strategy.

1 Introduction

The boundary layer flow over a porous laminated flat plate is investigated using experimental and computational methods to understand the flow dynamics at the fluid-porous interface. The existence of a slip velocity at this interface has been demonstrated through laboratory and numerical experiments (Beavers and Joseph, 1967; Brinkman, 1949; Larson and Higdon, 1987; Sangani and Yao, 1988; Tachie et al., 2003; Zhang and Prosperetti, 2009). However, the relationship of this slip velocity with the porous media or flow parameters is not elucidated. It was observed that an accurate understanding of the influence of the porous media parameters such as porosity (ϕ), thickness of the porous layer (h) etc. and the flow Reynolds number on the slip velocity at the fluid-porous interface is not reported in the available results. Hence, our aim is to understand the influence of the above parameters on the slip velocity and explore the scope of such porous laminations in flow separation control.

The problem has been extensively studied using analytical and numerical investigations, few among them being : Brinkman (1949); Saffman (1971); Taylor (1971); Larson and Higdon (1987); Sahraoui and Kaviany (1992); Ochoa-Tapia and Whitaker (1995); Zhang and Prosperetti (2009). Beavers and Joseph (1967) were the first to experimentally confirm the existence of slip velocity at the interface of the porous medium and the overlying free fluid layer. They conducted experiments using commercially available metal foams lined on one side of a rectangular channel and measured the flow rates inside the porous layer and in the free fluid layer at different pressure gradients across the channel. They proposed an *ad-hoc* boundary condition based on the intuition that the velocity gradient at the fluid-porous interface is proportional to the slip velocity, as

$$\left. \frac{\partial u}{\partial y} \right|_{y=0} = \frac{\alpha}{\sqrt{\kappa}} (U_{slip} - U_D) \quad (1)$$

where, α is a slip parameter, κ is the permeability of the porous medium, U_{slip} is the slip velocity at the fluid-porous interface and U_D is the Darcy velocity inside the porous medium. Their data was consistent with

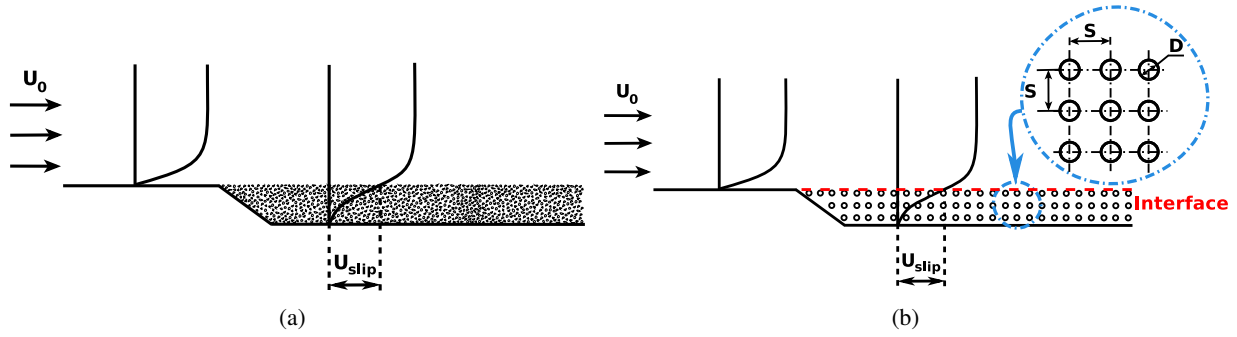


Figure 1: Illustration of the flow over the porous laminated flat plate with the slip velocity at the fluid-porous interface marked as, U_{slip} ; (a) schematic of actual porous lamination, (b) porous lamination modeled as array of cylinders.

the proposed boundary condition, Eqn. 1, but the value of α or its relationship with the porous parameters could not be determined. Beavers and Joseph (1967) suggested the randomness in the structure of the porous samples for the elusive definition of α and concluded that α is dependent solely on the structure of the porous medium. This motivated the modeling of porous media using simple in-line or staggered arrays of cylinders or rods of varying cross-sections and diameters as verified by the large number of later works (Saffman, 1971; Taylor, 1971; Larson and Higdon, 1987; Sangani and Yao, 1988; Sahraoui and Kaviany, 1992; Koch and Ladd, 1997; James and Davis, 2001; Tachie et al., 2003; Agelinchaab et al., 2006; Zhang and Prosperetti, 2009; Arthur et al., 2009).

The slip velocity at the fluid-porous interface is commonly modeled by adapting the boundary conditions to match the exterior free fluid flow (Beavers and Joseph, 1967; Saffman, 1971; Taylor, 1971; Larson and Higdon, 1987), or by the addition of stress equivalent terms in Darcy's law (Darcy, 1856) to match the order with that of Navier-Stokes equations (Brinkman, 1949; Sahraoui and Kaviany, 1992; Ochoa-Tapia and Whitaker, 1995). These two approaches are generally used in numerical and analytical investigations, which are found in abundance in literature. The experimental examination to infer the nature of the slip velocity has gained momentum in recent years with the advancement of optical measuring techniques. Gupte and Advani (1997) measured the local velocity profiles in a channel with a porous wall on one side, formed from strands of glass woven in random fashion, using Laser Doppler Anemometer (LDA) and confirmed the dependence of α on the porosity and microstructure of the porous medium, as reported by Beavers and Joseph (1967). Tachie et al. (2003) reported a decrease in slip velocity with decrease in porosity through PIV measurements at the fluid-porous interface on a Couette flow setup. They also found that the shape of the rods and the thickness of the porous layer had minimal influence on the slip velocity. A similar investigation by Agelinchaab et al. (2006) on a Poiseuille flow setup at low Re and $0.5 < \phi < 0.9$ confirmed the dependence of the slip velocity on the porosity, spacing between the rods and the filling fraction of the channel. In the same setup, Arthur et al. (2009) reported non-uniform velocity profiles for $\phi > 0.9$ due to greater flow interaction between the flow inside the porous layer and the overlying fluid layer. The PIV measurements of Goharzadeh et al. (2005), on a bed of mono-sized spheres, found that the gradient of slip velocity at the fluid-porous interface was a function of Re .

Almost all of the available results are for high ϕ ($\phi \gtrsim 0.8$) and low Re flows and are conducted on internal flows, whose results cannot be extrapolated to exterior flows due to the bounding wall boundary condition. In the present study, we conduct wind tunnel experiments to understand the relationship between the porous media parameters and the slip velocity in an exterior flow which constitutes majority of the fluid dynamic applications. We also carry out numerical simulations to investigate a larger range of ϕ and Re to substantiate our experimental analysis. The experimental and numerical methodologies are discussed in Sec. 2 and the key results are discussed in Sec. 3. We conclude and discuss the open questions in the conclusion.

2 Methodology

The reconstruction of porous media from its parameters such as porosity, permeability, inherent structural randomness etc. poses many challenges and hence, porous models are usually designed as square or staggered arrays of rods for both experimental and numerical analyses, as mentioned in Sec. 1. Figure 1 illus-

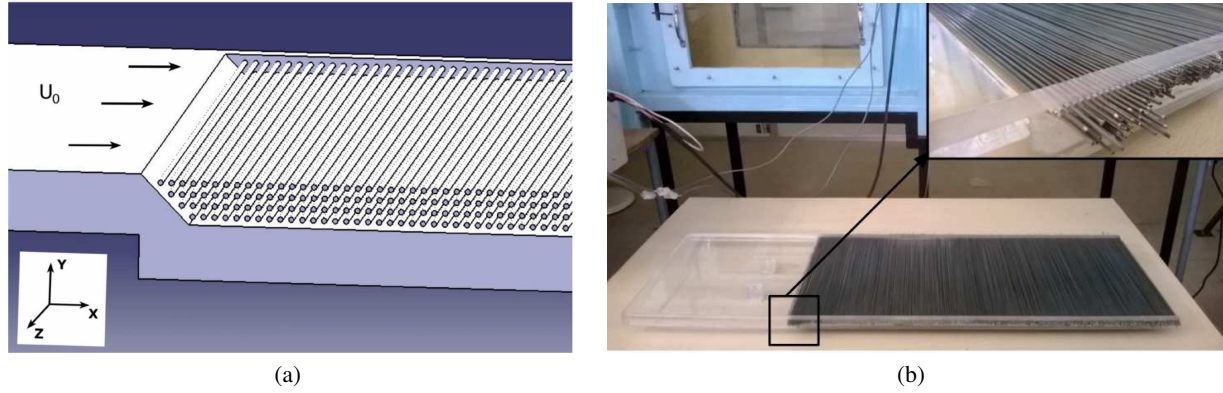


Figure 2: The experiment model of the porous laminated flat plate. (a) The 3D CAD model and, (b) the fabricated model.

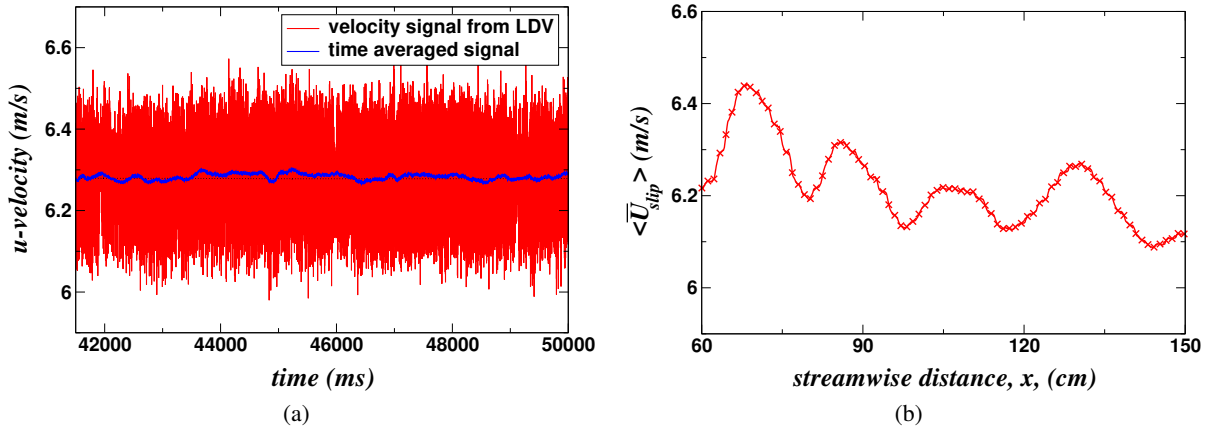


Figure 3: The velocity measurements for $\phi = 0.8$ at $Re = 391$: (a) The time series velocity signal measured by the LDV at the fluid-porous interface which shows the unsteady characteristic of the slip velocity at this Re . The unsteadiness increases with higher Re and ϕ . (b) The U_{slip} measured along the fluid-porous interface which has the spatial signature.

trates the predicted flow over the porous lamination and the modeling of this flow over the array of cylinders, with the slip velocity over the porous lamination marked in Fig. 1(a) and 1(b). The porosity of such models are calculated as $\phi = 1 - (\pi D^2/4)/S^2$, where the dimensions are as marked in Fig. 1(b). In the present study, the porous lamination is laid using a square array of 1586 circular rods of uniform diameter of 2 mm, placed transverse to the flow in the span-wise direction, as shown in Fig. 2(a) and 2(b). Figure 2(a) is the 3D model of the porous laminated flat plate, showing the reference axis of the problem and Fig. 2(b) shows the experiment model after fabrication. Only two models with porosities 0.65 and 0.8 were chosen for experiments due to difficulty in fabrication of models with lower porosity values.

The experiments are conducted in an open-loop, suction type, low noise wind tunnel with test section size of $0.5 \times 0.5 \times 2$ m. The speed range of the tunnel is 0 – 30 m/s. A one component Laser Doppler Velocimeter (1D LDV) probe is used for the velocity measurements due to its non-intrusive characteristics. The LDV measures the velocity at a single point in the flow field as a time series signal, as shown in Fig. 3(a), which is time averaged using appropriate averaging window. The lowest Re that can be investigated in the present setup is found to be $Re \sim 391$, based on the characteristic length of the porous model and the lowest velocity of the wind tunnel. The geometric structure of the porous lamination, moreover, introduces its spatial signature on the flow properties at the fluid-porous interface, as shown in Fig. 3(b). A spatial averaging of the flow properties, thus, becomes a necessity and an equivalent control volume known as the Representative Elementary Volume (REV) needs to be defined for a continuum analysis to be valid (Whitaker, 1966, 1985, 1999). The extensive exercise to determine the REV valid for the present study is explained in detail in Nair et al. (2018). We represent temporally averaged quantities with an over-line ($\bar{\cdot}$)

and REV -averaged quantities with angle brackets ($\langle \cdot \rangle$). The local and REV -averaged velocity profiles are measured for $Re = 391, 497$ and 803 .

The porosity and Re outside the scope of our experiments are analysed computationally to understand the nature of U_{slip} over a wider range of Re for different ϕ . The porosity values ranging from $\phi = 0.4$ to 0.9 are chosen as only high porosity values were found in the available literature. The problem is numerically analysed for Reynolds numbers of 25, 50, 75, 100, 150, 200, 250, 300, 500 and 1000, where Reynolds number is defined as, $Re = U_0 D / \nu$, where U_0 is the free-stream velocity, D is the diameter of the cylinders and ν is the kinematic viscosity. The computations are done using a hybrid Finite Element Method – Finite Volume Method (FEM-FVM) solver which solves the two-dimensional Navier-Stokes and continuity equations, details of the solver can be found in Kumar et al. (2016). The computational results are validated with the experiment results as no data is available in the literature for validation, which is discussed in Sec. 3.

3 Results and Discussion

We investigate the two-dimensional flow over a porous laminated flat plate with the aim of exploring the scope of porous laminations for separation control. The temporal and REV -averaged u -velocity profiles are plotted in Fig. 4(a), which clearly shows a significant non-zero slip velocity at the fluid-porous interface, thereby confirming the generation of a slip wall at the interface due to the porous lamination. The increasing nature of U_{slip} with ϕ can be clearly seen from the zoomed profiles in the inset of Fig. 4(a). An increase in porosity implies an increase in the gap between the cylinders and the fluid permeation into the porous layer increases through these wider gaps. This results in a rise in the tangential velocity at the fluid-porous interface, U_{slip} , to satisfy the continuity criterion. The plot of $\langle \overline{U}_{slip} \rangle$ with Re in Fig. 4(b) shows that at the experimentally examined ϕ and Re , $\langle \overline{U}_{slip} \rangle$ has a weak dependence on Re .

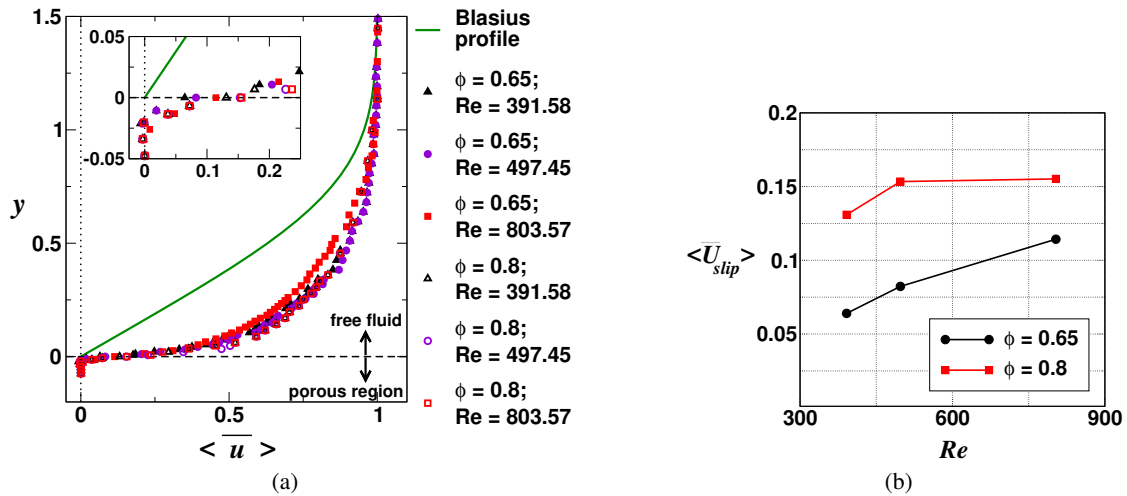


Figure 4: The velocity measurements for $\phi = 0.65$ & 0.8 at $Re = 391, 497$ & 803 . (a) The temporal and REV -averaged u -velocity profiles show a non-zero slip velocity at the fluid porous interface, which is marked with the dashed line. The zoomed view near the fluid-porous interface is shown in the inset. (b) The variation of $\langle \overline{U}_{slip} \rangle$ with Re shows that $\langle \overline{U}_{slip} \rangle$ has a weak dependence on Re at these ϕ & Re .

Figure 5 shows the comparison of the experimental and numerical data for the variation of $\langle \overline{U}_{slip} \rangle$ with Re , which confirms the weak dependence at higher ϕ and Re . It is presumed that at higher porosities, the effect of wider gap between the cylinders has a dominant influence on the flow dynamics at the fluid-porous interface than the increase in Re , which results in the weak dependence of Re on $\langle \overline{U}_{slip} \rangle$. Figure 5 also validates the numerical results with the experiment data showing similar trend, though there is a difference in the numerical values. The difference in values is attributed to the artifacts of the 3D nature of the experiments, minute surface imperfections in the experiment models etc. It has also been found that the vertical velocity at the fluid-porous interface alternated signs along the streamwise direction, resulting in an alternating passive suction-blowing phenomenon at the interface. This is the reason for the flatter velocity

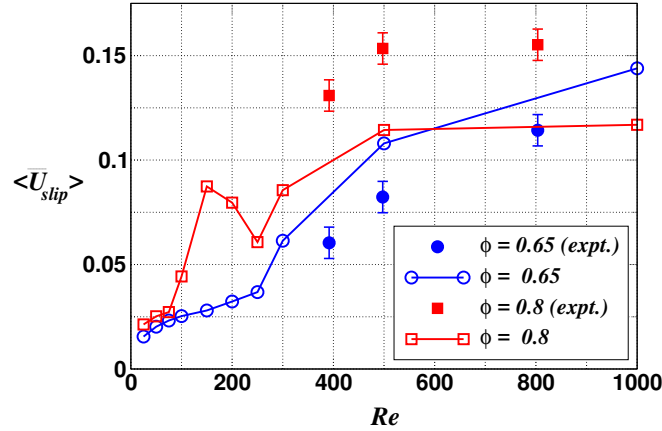


Figure 5: The comparison of experiment data with numerical results for the cases studied. The error bars represent measurement uncertainty at 95% confidence level. The variation in values is attributed to the 3D nature of the experiments, surface roughness of the rods etc..

profiles seen in Fig. 4(a), as suction effect is known to flatten the velocity profiles (Schlichting and Gersten, 2000). Further analysis of the numerical results revealed that the shear stress and pressure gradient along the interface promotes separation delay, which is analysed in detail in Nair et al. (2018). The existence of the slip wall along the fluid-porous interface and the flatter velocity profiles indicate that the porous lamination helps delay flow separation. This suggests the feasibility of porous laminations of high porosity ($\phi > 0.9$) for passive separation control.

4 Conclusion

The nature of the slip velocity at the fluid-porous interface had not been examined experimentally though a vast body of literature is available on its analytical and numerical investigations. The motivation for this study is the absence of the knowledge of flow physics at the fluid-porous interface, which could enhance the scope of porous laminations as a passive flow control technique. We conduct wind tunnel experiments to investigate the two-dimensional flow past a porous laminated flat plate with porosities 0.65 and 0.8 at $Re = 391, 497$ and 803 and measure the velocities at the fluid-porous interface using a 1D LDV. Numerical analysis is done for $0.4 < \phi < 0.9$ and $25 < Re < 1000$ to support the experimental analysis. We confirm the existence of a significant U_{slip} at the fluid-porous interface, which is a function of ϕ and Re . The U_{slip} shows unsteady and non-uniform characteristics at the experimentally investigated Re , which has been confirmed by the numerical results. An alternating passive suction-blowing phenomenon is, moreover, seen at the fluid-porous interface at higher ϕ and Re , which flattens the velocity profiles over the porous laminated regions. The presence of the slip wall and the flatter velocity profiles over the porous lamination are indications of separation delay. We, therefore, propose that a porous lamination with $\phi > 0.9$ could be effective as a passive separation control technique at higher Re for external flows.

Acknowledgements

The authors wish to thank the Aeronautical Research and Development Board (AR&DB), DRDO, Government of India, for the financial support towards the experimental analysis. The computations were done using facilities at the High Performance Computing Environment(HPCE) at IIT Madras.

References

Agelinchab M, Tachie MF, and Ruth DW (2006) Velocity measurement of flow through a model three-dimensional porous medium. *Physics of Fluids* 18:017105–1–11

- Arthur JK, Ruth DW, and Tachie MF (2009) PIV measurements of flow through a model porous medium with varying boundary conditions. *Journal of Fluid Mechanics* 629:343–374
- Beavers GS and Joseph DD (1967) Boundary conditions at a naturally permeable wall. *Journal of Fluid Mechanics* 30:197–207
- Brinkman HC (1949) A calculation of the viscous force exerted by a flowing fluid on a dense swarm of particles.. *Applied Scientific Research* A1:27–34
- Darcy H (1856) *Les Fontaines Publiques de la Ville de Dijon*. Dalmont
- Goharzadeh A, Khalili A, and Jorgensen B (2005) Transition layer thickness at a fluid-porous interface. *Physics of Fluids* 17:057102
- Gupte SK and Advani SG (1997) Flow near the permeable boundary of a porous medium: An experimental investigation using LDA. *Experiments in Fluids* 22:408–422
- James DF and Davis AMJ (2001) Flow at the interface of a fibrous porous medium. *Journal of Fluid Mechanics* 426:47–72
- Koch DL and Ladd AJC (1997) Moderate Reynolds number flow through periodic and random arrays of aligned cylinders. *Journal of Fluid Mechanics* 349:31–66
- Kumar SA, Mathur M, Sameen A, and Lal SA (2016) Effects of Prandtl number on the laminar cross flow past a heated cylinder. *Physics of Fluids* 28:113–603
- Larson RE and Higdon JJJ (1987) Microscopic flow near the surface of two-dimensional porous media. Part 2. Transverse flow. *Journal of Fluid Mechanics* 178:119–136
- Nair KA, Sameen A, and Lal SA (2018) Passive Boundary Layer Flow Control Using Porous Lamination. *Transport in Porous Media* (in press)
- Ochoa-Tapia JA and Whitaker S (1995) Momentum transfer at the boundary between a porous medium and a homogeneous fluid - I : Theoretical Development.. *International Journal of Heat and Mass Transfer* 38:2635–2646
- Saffman PG (1971) On the boundary condition at the surface of a porous medium. *Studies in Applied Mathematics* 50:93–101
- Sahraoui M and Kaviani M (1992) Slip and no-slip velocity boundary conditions at interface of porous, plain media. *International Journal of Heat and Mass Transfer* 35:927–943
- Sangani AS and Yao C (1988) Transport processes in random arrays of cylinders. II. Viscous Flow. *Physics of Fluids* 31:2435–2444
- Schlichting H and Gersten K (2000) *Boundary-Layer Theory*. Springer
- Tachie MF, James DF, and Currie IG (2003) Velocity measurements of a shear flow penetrating a porous medium. *Journal of Fluid Mechanics* 493:319–343
- Taylor GI (1971) A model for the boundary condition of a porous material. Part 1.. *Journal of Fluid Mechanics* 49:319–326
- Whitaker S (1966) The equations of motion in porous media. *Chemical Engineering Science* 21:291–300
- Whitaker S (1985) A simple geometrical derivation of the spatial averaging theorem.. *Chemical Engineering Education* 19
- Whitaker S (1999) *The method of Volume Averaging. Theory and Applications of transport in porous media*. Kluwer Academic Publishers
- Zhang Q and Prosperetti A (2009) Pressure-driven flow in a two-dimensional channel with porous walls. *Journal of Fluid Mechanics* 631:1–21